BAYESIAN SPARSE MODEL FOR COMPLEX-VALUED MAGNETIC RESONANCE SPECTROSCOPY RESTORATION

Wafae Labriji, Soléakhéna Ken, Gaelle Dormio, Jean-Yves Tourneret, Elizabeth Moyal Cohen-Jonathan, Lotfi Chaari

BAYESIAN SPARSE MODEL FOR COMPLEX-VALUED MAGNETIC RESONANCE SPECTROSCOPY RESTORATION

Wafae Labriji[1], *Soléakhéna Ken* [2,3], *Gaelle Dormio*[3], *Jean-Yves Tourneret*[1], *Elizabeth Moyal Cohen-Jonathan*[2,3] *and Lotfi Chaari*[1]

[1] Toulouse INP, University of Toulouse, IRIT, France
[2] Institut Universitaire du Cancer – Oncopole Claudius Regaud, 31059 Toulouse, France
[3] Centre de Recherches en Cancérologie de Toulouse, INSERM UMR1037, Equipe RADOPT

ABSTRACT

Sparse regularisation has proven its worth and effectiveness in many fields, such as medical imaging. In this sense, nuclear magnetic resonance spectroscopy (MRS) is one of the modalities that could greatly benefit from sparse regularisation. This paper introduces a novel Bayesian approach for MRS restoration that accounts for possible errors in the observation linear operator. The algorithm is tailored to the complex nature of MRS data, incorporating both real and imaginary parts of the spectrum. An MCMC (Markov chain Monte Carlo) inference is conducted using a Gibbs sampler strategy. The method has been successfully validated on both synthetic and clinical data of high-grade brain tumor glioblastoma (GBM) patients. This study will enable further analysis of metabolites of interest not conventionally considered in clinics because of their undetectable concentration.

1 Introduction

Brain magnetic resonance spectroscopy (MRS) is a powerful non-invasive exploration technique that provides highly valuable information on the biochemical composition and metabolic activity of the brain. Furthermore, MRS plays a crucial role in oncology, enabling clinicians to characterise tumors and even to target the therapy according to their metabolic abnormalities [1, 2].

However, the analysis of MRS data can be very challenging, mainly due to the inherently low signal-to-noise ratio (SNR). Among the most prevalent techniques, the linear combination model (LCM) fitting method is one of the most common approaches [3]. In this approach, the contribution of each metabolite to the overall spectrum is modelled using a dedicated response function known as a basis spectrum, which acts as the observation operator. Regarding LCM methods, based on inverse problem solving, there is a wide range of ready-to-use softwares relying on different algorithms, starting from the simple non-linear least-squares analysis [4] to approaches based on Bayesian inference [5].

Addressing the challenges of inverse problem resolution in brain MRS requires innovative methodologies that not only enhance the quantification of well-known metabolites but also open avenues for the discovery of hidden compounds not yet analysed because no method could detect their presence drowned in noise. One promising approach to overcome these challenges consists of promoting signal sparsity via Bayesian inference. This paper investigates a new method for sparse regularisation of MRS signals accounting for observation operator errors. The above-mentioned method has been previously proposed and validated for EEG (electroencephalogram data) [6, 7]. Modifications have been applied to adapt the algorithm to the nature of MRS data that are complex, which requires a specific processing. The proposed approach enables the estimation of both the target coefficients and the linear operator in the observation model. Meanwhile, the other model parameters and hyperparameters are automatically estimated from the available data. This involves the construction of a hierarchical Bayesian model using a specific likelihood and suitable priors. Finally, a Markov Chain Monte Carlo (MCMC) algorithm is used to generate samples that are asymptotically distributed according to the target distribution, ensuring highly reliable estimate for all the model parameters.

This paper is structured as follows. Section II introduces the proposed Bayesian method. Section III evaluates the performance of this method using synthetic and *in vivo* MRS imaging (MRSI) data. Finally, conclusions are presented in Section IV, where the findings are summarised and future perspectives are discussed.

2 Proposed Method

2.1 Problem formulation

Let $\boldsymbol{a} = (a_1, ..., a_M)^T \in \mathbb{R}_+^M$ be the target vector, containing the contribution of M metabolites to the observed signal, measured by $\boldsymbol{y} \in \mathbb{C}^P$ through a linear operator $\mathcal{H} \in \mathbb{C}^{P \times M}$. The operator $\mathcal{H}$ stands here for the metabolite basis set, where each column corresponds to the spectral pattern of a single metabolite. Accounting for the additive complex-valued acquisition noise $\boldsymbol{n} \in \mathbb{C}^P$, the observation model we are inter-

ested in can be written as:

$$\boldsymbol{y} = \mathcal{H}\boldsymbol{a} + \boldsymbol{n}. \quad (1)$$

Since all metabolites do not necessarily contribute to the measured spectrum $\boldsymbol{y}$, the metabolites contribution vector $\boldsymbol{a}$ is assumed to be sparse. We therefore aim to apply a sparse regularisation strategy to estimate the unknown coefficients of $\boldsymbol{a}$ in a Bayesian framework. More specifically, we propose to extend the Bayesian sparse regularisation method developed in [6] to the case of complex-valued signals, while also accounting for potential errors in the estimation of the linear operator $\mathcal{H}$ [7]. In this article, a Bernoulli-exponential distribution is proposed as *prior* for the target vector a and a Gaussian *prior* for the linear operator $\mathcal{H}$.

2.2 Hierarchical Bayesian model

In this section, we introduce the hierarchical Bayesian model employed, outlining both the chosen likelihood and priors.

2.2.1 Likelihood

Under the assumption of complex-valued additive Gaussian noise of covariance matrix $\Psi = \sigma_n^2 I$, the likelihood can be expressed as follows:

$$f(\boldsymbol{y}|\boldsymbol{a}, \sigma_n^2, \mathcal{H}) = \frac{1}{\pi^P \sigma_n^{2P}} \exp\left(-\frac{\|\boldsymbol{y} - \mathcal{H}\boldsymbol{a})\|^2}{\sigma_n^2}\right), \quad (2)$$

where $\|.\|$ is the ℓ_2 norm.

2.2.2 Priors

Bayesian inference requires to define prior information about the unknown model parameters, i.e., $\boldsymbol{a}$, σ_n^2 and $\mathcal{H}$. These priors are described in this section.

Target vector $\boldsymbol{a}$

Long echo-time spectroscopy (TE $\geq$ 130 ms) is often associated with sparse signals in the frequency domain. In order to promote the sparsity of the vector $\boldsymbol{a}$, a Bernoulli-exponential prior is assigned to each coefficient a_i leading to:

$$f(a_i|\omega, \lambda) = (1-\omega)\delta(a_i) + \frac{\omega}{\lambda}\exp\Big(-\frac{a_i}{\lambda}\Big)1_{\mathbb{R}_+^*}, \quad (3)$$

where $\delta(.)$ is the Dirac function, $\lambda > 0$ is the parameter of the exponential distribution, and ω is a weight in $]0, 1[$ that enables to control the proportion of zero coefficients. This prior has found widespread application in literature for the sparse reconstruction of noisy images and signals [8]. Assuming the prior independence of $a_1, ..., a_M$, the joint prior of $\boldsymbol{a}$ is:

$$f(\boldsymbol{a}|\omega, \lambda) = \prod_{i=1}^{M} f(a_i|\omega, \lambda). \quad (4)$$

Noise variance σ_n^2

To guarantee the positivity of σ_n^2 and keep this prior non-informative, a Jeffreys prior is assigned to σ_n^2:

$$f(\sigma_n^2) \propto \frac{1}{\sigma_n^2} 1_{\mathbb{R}_+}(\sigma_n^2), \quad (5)$$

where $1_{\mathbb{R}^+}(\xi) = 1$ if $\xi \in \mathbb{R}^+$ and 0 otherwise.

Operator $\mathcal{H}$

To account for possible inaccuracies in the observation operator $\mathcal{H}$, we adopt here a complex-valued Gaussian prior to the vectorized observation operator $\boldsymbol{h}$, with a diagonal covariance matrix $\Upsilon = \sigma_h^2 \mathbf{I}$ and mean $\bar{\boldsymbol{h}}$:

$$f(\boldsymbol{h}|\bar{\boldsymbol{h}}, \sigma_h^2) = \frac{1}{(\pi\sigma_h^2)^{PM}} \exp\left(-\frac{\|\boldsymbol{h} - \bar{\boldsymbol{h}}\|_2^2}{\sigma_h^2}\right). \quad (6)$$

This prior allows one to assume that the observation operator is close to its mean $\bar{\boldsymbol{h}}$, which is the reference basis set of metabolites quantified in the spectrum [9]. Note that $\bar{\boldsymbol{h}}$ is assumed to be known and that σ_h^2 is a hyperparameter, which will be estimated jointly with the other model parameters. The unknown parameter vector to be estimated is denoted by $\boldsymbol{\theta} = \{\boldsymbol{a}, \boldsymbol{h}, \sigma_n^2, \sigma_h^2\}$ in what follows.

2.2.3 Hyperparameter priors

Hyperprior on ω

A uniform distribution on the simplex $]0, 1[$ has been used for ω as a non informative prior, i.e., $\omega \sim \mathcal{U}_{]0,1[}(\omega)$.

Hyperprior on λ

Since λ is real positive, a conjugate inverse-gamma (IG) distribution has been used as a hyper-prior for this parameter:

$$f(\lambda|\alpha, \beta) = \mathcal{IG}(\lambda|\alpha, \beta) = \frac{\beta^\alpha}{\Gamma(\alpha)}\lambda^{-\alpha-1}\exp\left(-\frac{\beta}{\lambda}\right), \quad (7)$$

where $\Gamma(.)$ is the gamma function, while α and β are hyperparameters set to $\alpha = \beta = 10^{-3}$. These values of α and β ensure a non-informative prior for λ.

Hyperprior on σ_h^2

A Jeffreys' prior is assigned to σ_h^2 (as for σ_n^2):

$$f(\sigma_h^2) \propto \frac{1}{\sigma_h^2} 1_{\mathbb{R}_+}(\sigma_h^2). \quad (8)$$

2.3 Bayesian inference scheme

We adopt here a Maximum A Posteriori (MAP) strategy in order to estimate the model parameters vector $\boldsymbol{\theta}$ based on the likelihood, the priors and hyperpriors introduced here-above. Denoting as $\boldsymbol{\Phi} = \{\lambda, \omega, \sigma_h^2\}$ the hyperparameter vector, the posterior distribution of $\{\boldsymbol{\theta}, \boldsymbol{\Phi}\}$ writes:

$$f(\boldsymbol{\theta}, \boldsymbol{\Phi}|\boldsymbol{y}, \alpha, \beta) \propto f(\boldsymbol{y}|\boldsymbol{\theta}) f(\boldsymbol{\theta}|\boldsymbol{\Phi}) f(\boldsymbol{\Phi}|\alpha, \beta). \quad (9)$$

Assuming independence between the model parameters, the conditional distribution $f(\boldsymbol{\theta}|\boldsymbol{\Phi})$ can be derived from the product of distributions (4), (5) and (8). Akin to [6, 7], we propose to use a Gibbs algorithm to iteratively sample according to the conditional distributions of (9), i.e., $f(\boldsymbol{a}|\boldsymbol{y}, \omega, \lambda, \boldsymbol{h}, \sigma_n^2)$, $f(\sigma_n^2|\boldsymbol{y}, \boldsymbol{a}, \boldsymbol{h})$, $f(\boldsymbol{h}|\sigma_h^2, \boldsymbol{y}, \boldsymbol{a})$ $f(\lambda|\boldsymbol{a}, \alpha, \beta)$, $f(\omega|\boldsymbol{a})$, $f(\sigma_h^2|\boldsymbol{h})$. The conditional distributions $f(\lambda|\boldsymbol{a}, \alpha, \beta)$ and $f(\omega|\boldsymbol{a})$ are the same as in [6], whereas $f(\sigma_n^2|\boldsymbol{y}, \boldsymbol{a}, \boldsymbol{h})$ and $f(\sigma_h^2|\boldsymbol{h})$ are the following inverse gamma distributions:

$$\begin{aligned} \sigma_n^2|\boldsymbol{y}, \boldsymbol{a}, \boldsymbol{h} &\sim \mathcal{IG}(\sigma_n^2|P, \|\boldsymbol{y} - \mathcal{H}\boldsymbol{a}\|_2^2), \\ \sigma_h^2|\boldsymbol{h} &\sim \mathcal{IG}(\sigma_h^2|PM, \|\boldsymbol{h} - \bar{\boldsymbol{h}}\|_2^2). \end{aligned} \quad (10)$$

2.3.1 Sampling according to $f(\boldsymbol{h}|\sigma_h^2, \boldsymbol{y}, \boldsymbol{a})$

Decomposing $\boldsymbol{h}$ on the orthonormal basis $\{\boldsymbol{V}_1, \cdots, \boldsymbol{V}_{\text{MP}}\}$ such that $\boldsymbol{h} = \boldsymbol{h}_{-l} + \boldsymbol{h}_l \boldsymbol{V}_l$, where $\boldsymbol{h}_{-l}$ stands for $\boldsymbol{h}$ where $\boldsymbol{h}_l$ has been set to 0, straightforward calculations yield the following conditional distribution for $\boldsymbol{h}_l$:

$$\boldsymbol{h}_l|\boldsymbol{a}, \boldsymbol{y}, \sigma_n^2, \boldsymbol{h}_{-l}, \bar{\boldsymbol{h}}, \sigma_h^2 \sim \mathcal{N}(\mu_l, \sigma_l^2), \tag{11}$$

where $\sigma_l^2 = \frac{\sigma_h^2 \sigma_n^2}{\sigma_n^2 + \sigma_h^2 a_l^2}$, $\mu_l = \sigma_l^2 \left(\frac{\bar{h}_l}{\sigma_h^2} + \frac{\boldsymbol{a}^\intercal \mathbf{V}_l^\intercal \boldsymbol{z}_l}{\sigma_n^2} \right)$, $\boldsymbol{z}_l = \boldsymbol{y} - \boldsymbol{h}_{-l}^\intercal \boldsymbol{a}$ and $^\intercal$ means "transpose conjugate".

2.3.2 Sampling according to $f(\boldsymbol{a}|\boldsymbol{y}, \omega, \lambda, \boldsymbol{h}, \sigma_n^2)$

Decomposing $\boldsymbol{a}$ on the orthonormal basis $\{U_1, \ldots, U_M\}$ such that $\boldsymbol{a} = \boldsymbol{a}_{-i} + a_i U_i$, where $\boldsymbol{a}_{-i}$ is the vector $\boldsymbol{a}$ whose ith element has been set to 0, straightforward calculations, as those performed in [8], lead to the conditional distribution:

$$\begin{aligned} &f(a_i|\omega, \lambda, \sigma^2, \boldsymbol{a}_{-i}, \boldsymbol{y}, \boldsymbol{h}) \\ &\quad = \omega_{0,i}\delta(a_i) + \omega_{1,i}\Psi^+(a_i, \mu_i, \sigma_i^2). \end{aligned} \tag{12}$$

The resulting distribution is a truncated Bernoulli Gaussian distribution with a mean μ_i and a variance σ_i^2, given by:

$$\Psi^+(a_i, \mu_i, \rho_i) = \frac{1}{C(\mu_i, \rho_i)} e^{-\frac{(a_i - \mu_i)^2}{2\rho_i}},$$

where:
$$C(\mu_i, \rho_i) = \sqrt{\frac{\pi \rho_i}{2}} \left[1 + \text{erf}\left(\frac{\mu_i}{\sqrt{2\rho_i}} \right) \right],$$

and μ_i and ρ_i are given by:

$$\rho_i = \frac{\sigma_n^2}{\|\mathbf{h_i}\|^2}, \quad \text{and} \quad \mu_{l,i} = \rho_i \left(\frac{\mathbf{e_i}^\intercal \mathbf{h_i}}{\sigma_n^2} + \frac{\mathbf{h_i}^\intercal \mathbf{e_i}}{\sigma_n^2} - \frac{1}{\lambda} \right),$$

where $\mathbf{h_i} = \mathcal{H}\mathbf{U_i}$ and $\mathbf{e_i} = \boldsymbol{y} - (\mathcal{H}\boldsymbol{a} - \mathcal{H}_i a_i \mathbf{U_i})$.
Moreover, the weights $(\omega_{l,i})_{0 \le l \le 1}$ in (12) are defined by

$$\omega_{l,i} = \frac{u_{l,i}}{u_{0,i} + u_{1,i}},$$

with $u_{0,i} = 1 - \omega$ and $u_{1,i} = \sqrt{2\pi\rho_i} \frac{\omega}{\lambda} \exp\left(\frac{\mu_i^2}{2\rho_i} \right) C(\mu_i, \rho_i)$.
As regards the general Gibbs sampler, an algorithm similar to [7] is used so sample according to the above-detailed distributions. After the burn-in period, an MMSE (Minimum Mean Square Error) estimator is used to estimate the unknown model parameters.

3 Simulation results

The results of proposed method (referred to as MCMC) were obtained by considering 600 iterations, 300 of which were burn-ins. The implementation was carried out in Matlab R2023b on a 5.20GHz i7-1365U processor with 64GB RAM. Each estimation required 30 seconds.

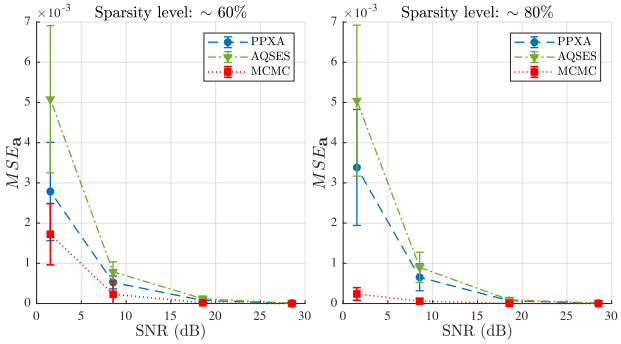

Fig. 1: MSE of estimated metabolite amplitudes (10 MC runs).

3.1 Synthetic data

In order to evaluate the performance of the proposed method (referred to as MCMC), we conducted a first experiment on synthetic data, obtained by combining the profiles [9] of the metabolites potentially present in the brain. Simulated spectra were obtained according to the observation model in (1) using proportions of these metabolites. Four different levels of complex white Gaussian noise were used. For each noise level, $N = 10$ Monte-Carlo runs were performed to assess mean and variance accuracy to recover the original metabolite proportions $\boldsymbol{a}$. For the sake of comparison, MCMC is compared to two state of the art methods: variational regularization using a Parallel Proximal Algorithm (PPXA) [10] and the well-known AQSES method [4] based on a least-squares criterion. To investigate the ability of the proposed method to recover accurate sparsity levels, Table 1 reports the l_0 pseudo-norm values of $\boldsymbol{a}$ for the different input SNRs and sparsity levels. These figures confirm the ability of the proposed method to accurately recover the sparsity level of the ground truth data. The mean squared errors (MSE) of the estimated metabolite proportion vectors $\boldsymbol{a}$ computed using 10 Monte-Carlo runs are shown in Figure 1 for different SNRs and sparsity levels. These results demonstrate the high performance of the MCMC method to estimate individual metabolite amplitudes. The values of $\text{MSE}_{\boldsymbol{a}}$ obtained using the MCMC method are systematically lower than those obtained with the state-of-the-art, for the different SNR levels of SNR, even at the lowest signal sparsity level. Regarding the l_0-norm, the MCMC method is able to retrieve the correct number of non-zero coefficients under high to medium SNRs, and with reasonable uncertainty under low SNRs (Table 1).

		Input SNR			
Sparsity Level	$\|\|\boldsymbol{a}_{\text{ref}}\|\|_0$	28.5 dB	18.6 dB	8.5 dB	1.5 dB
60%	7	7	7	7± 0.5	6.3 ± 0.7
80%	4	4	4	4.1 ± 0.3	4

Table 1: l_0 pseudo-norm of the estimated amplitude vector versus the sparsity level and the SNR of the synthetic signal: mean and standard deviation over 10 MC runs.

3.2 *In-vivo* data

For *in-vivo* data, appropriate approvals were obtained from the relevant ethics committees and the French competent au-

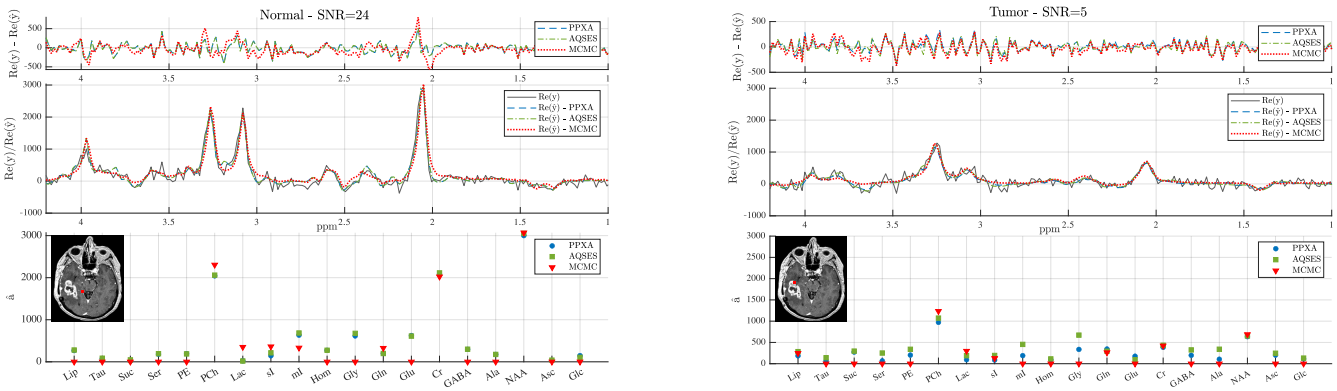

Fig. 2: Two representative spectra from a GBM patient and the corresponding estimations using PPXA, AQSES and MCMC. Metabolites of interest were: *Asc*: Ascorbic Acid, *Cr*: Creatine, *GABA*: γ-Aminobutyric Acid, *Glc*: Glucose, *Gln*: Glutamine, *Glu*: Glutamate, *Gly*: Glycine, *Hom*: Homocarnosine, *Lac*: Lactate, *Lip*: Lipids, *NAA*: N-Acetyl Aspartate, *PCh*: Phosphocholine, *PE*: Phosphorylethanolamine, *Ser*: Serine, *Tau*: Taurine, *2HG*: 2-Hydroxyglutarate, *Glc*: Glucose, *mI*: myo-Inositol, *sI*: scyllo-Inositol.

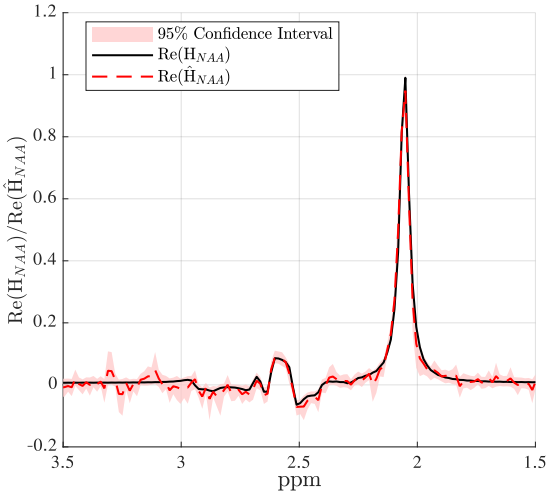

Fig. 3: Estimated observation operator for the *NAA* metabolite compared with the reference basis spectrum obtained from the normal voxel processing (Fig. 2).

thority. All enrolled patients gave their written informed consent. We tested the proposed method on *in-vivo* MRSI data from a GBM patient acquired after surgery and before chemoradiotherapy. We show the results for two representative voxels: normal tissue and contrast enhancing tumor (red squares in the left and right MR images of Fig. 2). For each voxel, the SNR was computed from the ratio between the *NAA* peak intensity in the spectrum modulus and the noise standard deviation (calculated in a metabolite-free region (> 5 ppm)) [11].

A number of observations can be drawn from the analysis of the spectra using the proposed MCMC method and the other two state-of-the-art methods (Fig. 2). From a clinical perspective, the obtained results are consistent with brain tumor state of the art [12]. In the tumor, a decrease in *NAA* and Creatine was detected, along with a significant increase in Choline, indicating a cellular proliferation. Moreover, clinical data analysis reveals the significant differences in SNR depending on the voxel location, and highlights the need for a noise-robust quantification method. This difference in SNR can be mainly attributed to the collapse of *NAA* peak due to functional neurons decrease and residual tumor activity; and possibly as a result of post-surgical reshaping and magnetic field heterogeneity. The three methods performed similarly when it came to quantifying metabolites abundantly present in the brain (*NAA*, *Cr*, *Cho* and *Lac*/*Lip* when available). However, the MCMC method performs more consistently with the sparse nature of MR spectra at long echo-time with a lower number of non-zero coefficients (for both voxels: $\|\hat{\boldsymbol{a}}\|_0 = 7$). An example of the estimated operator for *NAA* metabolite with MCMC is given in Fig. 3, demonstrating the ability to correct for small imperfections in the reference operator while maintaining close alignment with it. Yet, it's important to note that comparing various methods using *in-vivo* data without a definitive reference point is challenging. Future research involving synthetic data should integrate additional elements mirroring real-world artifacts [11], which are essential for producing results that can be more easily transposable to *in-vivo* data.

4 Conclusion

In this paper, we have adapted a Bayesian method for sparse signal regularisation to complex-valued MRS data. The method has been successfully validated on synthetic signals as well as clinical data, for which an expert validated the spectra fitting. This work opens the way to a number of perspectives, in particular the quantification of minor metabolites, present in low concentrations in the brain but likely to be affected by the patient's condition. As part of the project, this method will be applied to the follow-up of GBM patients and analysed alongside with blood metabolism of patients' samples taken at the same time points.

5 References

[1] S. Ken, L. Vieillevigne, and X. et al. Franceries, "Integration method of 3D MR spectroscopy into treatment planning system for glioblastoma IMRT dose painting with integrated simultaneous boost," *Radiation oncology*, vol. 8, pp. 1–9, 2013.

[2] A. Laruelo, L. Chaari, H. Batatia, S. Ken, B. Rowland, J.-Y. Tourneret, and A. Laprie, "Hybrid sparse regularization for magnetic resonance spectroscopy," in *IEEE International Conference of Engineering in Medicine and Biology Society (EMBC)*, Osaka, Japan, July, 3-7 2013.

[3] J. Near, A. D. Harris, C. Juchem, R. Kreis, M. Marjańska, G. Öz, J. Slotboom, M. Wilson, and C. Gasparovic, "Preprocessing, analysis and quantification in single-voxel magnetic resonance spectroscopy: experts' consensus recommendations," *NMR in Biomedicine*, vol. 34, no. 5, pp. e4257, 2021.

[4] J.-B. Poullet, D. M. Sima, A. W. Simonetti, B. De Neuter, L. Vanhamme, P. Lemmerling, and S. Van Huffel, "An automated quantitation of short echo time MRS spectra in an open source software environment: AQSES," *NMR in Biomedicine*, vol. 20, no. 5, pp. 493–504, 2007.

[5] W. T. Clarke, C. J. Stagg, and S. Jbabdi, "FSL-MRS: An end-to-end spectroscopy analysis package," *Magnetic resonance in medicine*, vol. 85, no. 6, pp. 2950–2964, 2021.

[6] L. Chaari, J.-Y. Tourneret, and H. Batatia, "Sparse Bayesian regularization using Bernoulli-Laplacian priors," in *EUSIPCO*, Marrakech, Morocco, September, 9-13 2013.

[7] L. Chaari, H. Batatia, and J.-Y. Tourneret, "Sparse Bayesian image restoration with linear operator uncertainties with application to EEG signal recovery," in *2nd MECBME*. IEEE, 2014, pp. 139–142.

[8] N. Dobigeon, A. O. Hero, and J.-Y. Tourneret, "Hierarchical Bayesian sparse image reconstruction with application to MRFM," *IEEE trans. on IP*, vol. 18, no. 9, pp. 2059–2070, 2009.

[9] M. Gajdošík, K. Landheer, K. M. Swanberg, and C. Juchem, "Inspector: free software for mrs data inspection, processing, simulation and analysis," *Scientific reports*, vol. 11, no. 1, pp. 2094, 2021.

[10] P. L. Combettes and J.-C. Pesquet, "A proximal decomposition method for solving convex variational inverse problems," *Inverse problems*, vol. 24, no. 6, pp. 065014, 2008.

[11] R. Kreis, "Issues of spectral quality in clinical 1h-magnetic resonance spectroscopy and a gallery of artifacts," *NMR in Biomedicine*, vol. 17, no. 6, pp. 361–381, 2004.

[12] M. Galijasevic, R. Steiger, S. Mangesius, J. Mangesius, J. Kerschbaumer, C. F. Freyschlag, N. Gruber, T. Janjic, E. R. Gizewski, and A. E. Grams, "Magnetic resonance spectroscopy in diagnosis and follow-up of gliomas: State-of-the-art," *Cancers*, vol. 14, no. 13, pp. 3197, 2022.